

CHARACTERIZATION OF PRESSURE DRIVEN AND ELECTRO-KINETICALLY DRIVEN FLOW IN A MICRO-FLUIDIC CHIP USING PARTICLE IMAGING VELOCIMETRY

A Senior Project

Presented to

the Faculty of the Materials Engineering Department
California Polytechnic State University, San Luis Obispo

In Partial Fulfillment

of the Requirements for the Degree
Bachelor of Science in Materials Engineering

by

Alexis Weckel

Project Title: Particle Imaging Velocimetry of a Pressure-Driven and Electro-Kinetically Driven Micro-Fluidic Chip

Author: Alexis Weckel

Date Submitted: June 6, 2014

CAL POLY STATE UNIVERSITY
Materials Engineering Department

Since this project is a result of a class assignment, it has been graded and accepted as fulfillment of the course requirements. Acceptance does not imply technical accuracy or reliability. Any use of the information in this report, including numerical data, is done at the risk of the user. These risks may include catastrophic failure of the device or infringement of patent or copyright laws. The students, faculty, and staff of Cal Poly State University, San Luis Obispo cannot be held liable for any misuse of the project.

Dr. Richard Savage
Thesis Advisor

Signature

Dr. Trevor Harding
Faculty Advisor

Signature

Dr. Katherine Chen
Department Chair

Signature

Table of Contents

| | |
|--|------|
| List of Tables | v |
| List of Figures | vi |
| Abstract | viii |
| Keywords | ix |
| Introduction & Background | 1 |
| Definition | 1 |
| History | 2 |
| Components of a Device | 2 |
| Micro-Filters | 2 |
| Micro-Needles | 3 |
| Micro-Mixers | 4 |
| Micro-Separators | 5 |
| Applications | 5 |
| Medical Diagnostics | 5 |
| Genetic Sequencing | 6 |
| Chemistry Production | 6 |
| Drug Discovery | 6 |
| Proteomics | 7 |
| Materials in Use | 7 |
| PDMS | 7 |
| Glass | 9 |
| Methods of Flow | 10 |
| Determining Type of Flow | 10 |
| Flow Driven By Capillary Forces | 12 |
| Pressure Driven Flow | 13 |
| Electro-Kinetic Forces | 14 |
| Measuring Velocity | 17 |
| Laser Doppler Velocimetry (LDV) | 18 |
| Molecular Tagging Velocimetry (MTV) | 19 |
| Particle Image Velocimetry (PIV) | 19 |
| Societal Impact | 20 |
| Project Definition/Research Question | 21 |
| Experimental Procedures | 22 |
| Fabrication Procedure | 22 |

| | |
|--|----|
| SU-8..... | 23 |
| PDMS | 23 |
| Plasma Bonding..... | 23 |
| Testing Procedure | 24 |
| Microscope Parameters | 24 |
| Pressure-Driven Flow Setup | 25 |
| Electro-Kinetic Flow Setup..... | 25 |
| Results and Analysis | 26 |
| Pressure-Driven Results | 27 |
| Syringe Pump Verification..... | 29 |
| Electro-Kinetic Results | 30 |
| Conclusions & Recommendations..... | 32 |
| Acknowledgments | 33 |
| References | 34 |
| Appendices..... | 36 |
| A. Fabrication Procedure | 36 |
| Cleaning..... | 36 |
| SU-8 Processing | 36 |
| PDMS Processing..... | 39 |
| Final Assembly..... | 40 |
| B. JMP Output for Pressure-Driven Data | 42 |
| 0.5 μ L/min | 44 |
| 0.75 μ L/min | 45 |

List of Tables

| | | |
|----------|--|----|
| Table I | Comparison chart of four main types of electro-kinetics..... | 14 |
| Table II | Pressure-driven results summary..... | 29 |

List of Figures

| | | |
|-----------|--|----|
| Figure 1 | Typical A) membrane filter designs and B) gap filter designs [4]. | 3 |
| Figure 2 | Designs of solid micro-needles [5]. | 4 |
| Figure 3 | Diffusion in a passive micro-mixer [1]. | 5 |
| Figure 4 | Structure of PDMS [1]. | 8 |
| Figure 5 | Processing of a PDMS microfluidic chip [1]. | 9 |
| Figure 6 | A) Unit cell and B) amorphous structure of glass [12]. | 10 |
| Figure 7 | Polar fluid in a hydrophobic channel [14]. | 12 |
| Figure 8 | Streaming potential in a channel [16]. | 15 |
| Figure 9 | Electro-osmotic flow in a channel [17]. | 17 |
| Figure 10 | Set-up of a laser Doppler velocimeter [19]. | 19 |
| Figure 11 | Schematic of components of a laser confocal microscope [21]. | 20 |
| Figure 12 | A) Mask used for fabrication of pressure-driven channels. The top channel was used with dimensions of 1mm wide and 25mm long. B) Mask designed in AutoCAD for fabrication of electro-kinetic channels. Channel dimensions are 170 μ m wide and 25mm long. The wells are 5mm squares. | 22 |
| Figure 13 | Process flow chart for the fabrication of PDMS channels. | 23 |
| Figure 14 | Setup of pressure-driven flow channel. | 25 |
| Figure 15 | Setup of electro-kinetic flow channel. | 26 |
| Figure 16 | Example overlay of 8 images in different colors to allow for PIV measurements. | 27 |
| Figure 17 | Time-lapse color coder used to analyze stacks of 8 images that had been overlaid in different colors. | 27 |
| Figure 18 | Pressure-driven results for 0.5 μ L/min (blue) and 0.75 μ L/min (red). For a wide and flat channel the parabolic profile would only be apparent near the wall of the channel (black). | 28 |
| Figure 19 | Setup for syringe pump verification. | 29 |

| | |
|---|----|
| Figure 20 Results of syringe pump verification. | 30 |
| Figure 21 Bubble traveling through the channel with 0.25 μ L/min of pressure and 50V. The voltage appears to have no impact on the flow. | 31 |
| Figure 22 This graph shows how spin speed related to film thickness of SU-8 2050 at Cal Poly in the past. This can be used to determine spinning parameters to obtain required thicknesses of SU-8 [24]. | 39 |
| Figure 23 These graphs can be used to determine spinning parameters for PDMS on the cover-slide. A) Different PDMS spin speeds for a 60 second spin. B) Different PDMS spin times for a 3000rpm spin speed [25]. | 42 |
| Figure 24 JMP output for 0.5 μ L/min of flow pressure. The edge is within 300 μ m of the wall. There is no significant difference between the regions of the channel. | 44 |
| Figure 25 JMP output for 0.75 μ L/min of flow pressure. The edge is within 300 μ m of the wall. No significant difference between the regions of the channel was found. | 45 |

Abstract

The goal of this research is to compare electro-kinetic and pressure driven flow rates and velocity profiles (near wall vs. middle) in a microfluidic chip made of PDMS using particle imaging velocimetry (PIV) of an aqueous solution of fluorescent polystyrene (PS) particles using a laser confocal microscope (LCM). Microfluidic channels were fabricated out of PDMS using a SU-8 mold to be 25mm long and 180 μ m by 1000 μ m. Pressure-driven data did not show the expected parabolic profile because of the large width to depth ratio. In addition, data showed a calculated average significantly higher than the projected particle velocity through the channel. Unexpected results were hypothesized to be caused by inaccuracies with the syringe pump or interactions with the tubing. The accuracy of the syringe pump was tested and found to be 20% lower for 0.5 μ L of flow and 4% lower for 0.75 μ L of flow, making the data even stranger. However, at the low pump rates the syringe pump was pulsing instead of having a consistent flow. This could have led to the inconsistencies seen. Other issues occurred when measuring electro-kinetic flow. Often flow would switch directions at random intervals, possibly due to some kind of charge build up. In addition, bubbles, possibly introduced into the system when connecting tubing or when moving the channel, were very problematic. Changes in temperature, pressure, surface properties of the channel, and properties of the fluid within the channel can cause bubbles to grow. Research suggested a bubble trapping method for temporary relief of keeping bubbles out of the channel. This research will be continued as my master's thesis next year.

Keywords

Materials

PDMS

Glass

Microfluidics

Pressure-Driven

Electro-Kinetics

Laser Confocal Microscope

Florescent Polystyrene Particles

Velocity Profile

Bubbles

Introduction & Background

Definition

Microfluidics deals with the flow of fluids, either gases or liquids, in channels with a least one dimension less than 100 micrometers. The flow in these channels differs from macro-scale fluid flows due to laminar flow.

There are natural channels on the micro-scale, but normally the term microfluidics refers to human-made objects. Microfluidic chips, a group of channels, can be etched or molded into a variety of materials as described in Section V. Different connections between the channels perform different functions. The channels are normally connected to the outside world through input and output holes and other connections to direct flow [1].

Microfluidics technology developed out of the semiconductor industry, so much of the processing is based on the processing of silicon. However, microfluidic channels can also be made of glass, ceramics, metals, and polymers because of newer processing steps. Materials are chosen based on compatibility, production time, costs, and the final application. PDMS (poly dimethyl siloxane), detailed in Section V Part A, is often used in research because of its low cost and quick processing [1].

History

The semiconductor industry has launched many spinoff technologies, including microfluidics. In the 1980's, silicon etching processes were developed that allowed the production of cantilever and diaphragms, also called MEMS (micro electromechanical systems) used in many sensory applications [2]. In the 1990's, research was done to use these systems as diagnostic tools in biology and chemistry mainly for use in hospitals, leading to the development of microfluidic systems, also called lab on a chip. This research expanded with the use of PDMS because of its low costs and quick production [1].

Components of a Device

Common microfluidic components include filters, needles, mixers, and separators [3].

Micro-Filters

Filters separate either large or small molecules based on physical size. Filter designs consider the distribution of the filtered particles, the pressure loss due to the filtering, and the mechanical strength of the filter to prevent break down over time. The two main types of filters used in microfluidics are membrane filters and gap filters (Figure 1) [4].

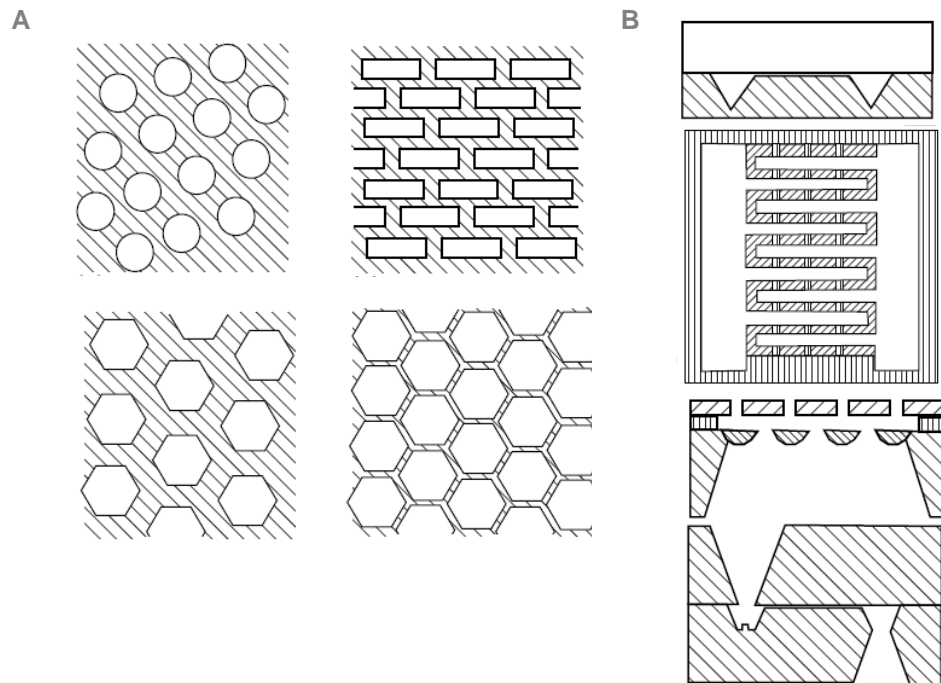


Figure 1 Typical A) membrane filter designs and B) gap filter designs [4].

Micro-Needles

Mainly used in the medical industry to deliver medication, micro-needles are a painless way of administering drugs. They are painless because they pierce the first layer of skin but do not penetrate to the nerves. In addition, these micro-needles do not require specialized personnel to administer. Designs consider the strength of the needles, the material's biocompatibility, and the flow of the medication through the needle. Potential problems include breaking of the needles within the skin causing irritation, slower flow of medication into the system, and greater chance of infection because of the multiple puncture sites. The drug could be in a reservoir under the needle, coated on the surface of the needle, or dissolved within the needle material incorporating either solid or hollowed needles (Figure 2) [5].

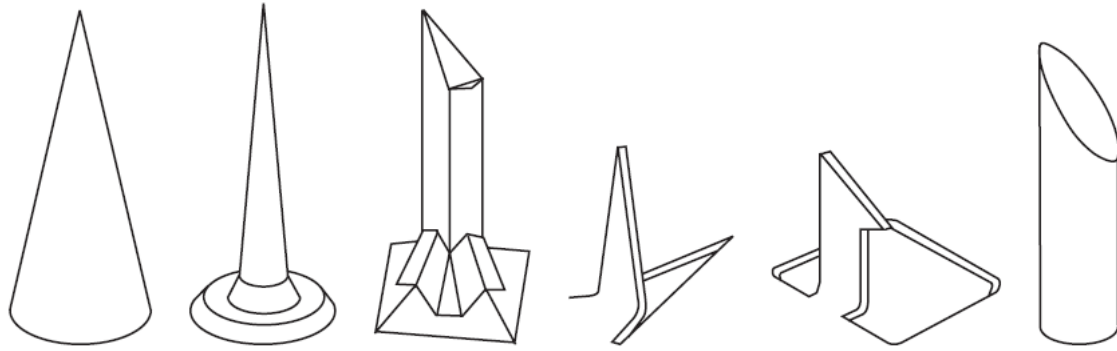


Figure 2 Designs of solid micro-needles [5].

Micro-Mixers

There are two types of micro-mixers: those with moving parts, active micro-mixers, and those without, passive micro-mixers. In both types, mixing is controlled by diffusion, which can be modeled by Fick's first and second laws (Figure 3). Fick's first law relates diffusion rate and concentration while Fick's second law relates concentration and time. Bends and obstacles can be added to a path to assist in mixing for passive micro-mixers. T-mixers and Y-mixers are common examples of passive micro-mixers. To increase passive mixing, multiple streams can be put into a passive mixer to increase the surface area over which diffusion occurs. Pressure, voltage potentials and micro-stirrers can be added to active micro-mixers to assist in mixing [5].

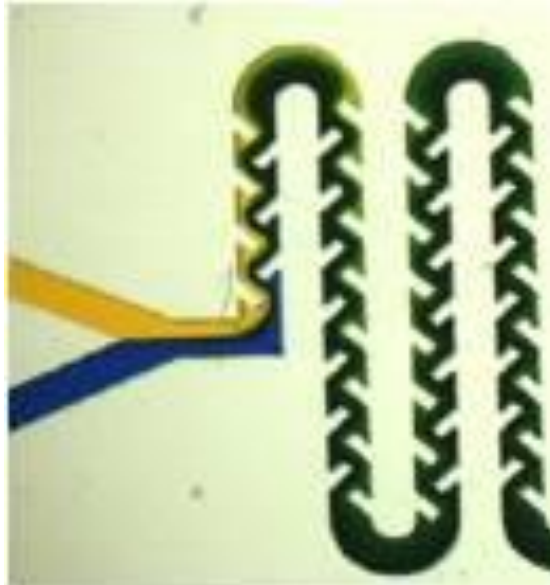


Figure 3 Diffusion in a passive micro-mixer [1].

Micro-Separators

Separators isolate particles based on properties. Particles can be separated based on properties other than size, like electrical and magnetic properties [4].

Applications

Researchers from many different fields of engineering and science are actively pursuing topics in microfluidics. The five major commercial applications of microfluidics are medical diagnostics, genetic sequencing, chemistry production, drug discovery, and proteomics [3].

Medical Diagnostics

Microfluidic devices are being developed to detect viruses and bacteria. These detection devices require smaller samples, less output time, and less lab work

than traditional diagnostic approaches, getting treatments to people faster [6]. In addition, multiple tests can be run simultaneously on the same device.

Genetic Sequencing

DNA sequencing on the macro-scale requires amplification, a process that copies the DNA strands by denaturing, annealing, and extension. Denaturing splits the DNA strands. Annealing and extension create the complimentary strands. The DNA strand is then separated and sequenced using various techniques. On the micro-scale, the main benefits are less reagent costs due to smaller volumes, quicker heating, quicker reaction times, laminar flow allowing the use of electro-osmotic or capillary flow, and precisely defined volumes. However, possible problems include samples degrading or evaporating [7].

Chemistry Production

Chemist and chemical engineers work to create industry scale reactions to create products from available materials. Currently, processes involve scaling-up which reduces precision and can be expensive. Microfluidics will allow for new reaction mechanisms. In addition, putting multiple chips in a sequence allows for interchangeable pieces creating customizable reactions from pre-manufactured items [8].

Drug Discovery

Drugs are being developed all the time for different ailments; however, about a decade of testing is required before reaching the market. Through microfluidics,

the new drugs can be analyzed more precisely and quickly using smaller amounts of reagents. However, these devices need to be versatile for multiple drug types and multiple testing situations. These devices can also be used to determine the correct dosage [9].

Proteomics

Proteomics is the study of proteins, which involves identifying the protein (profile), determining the purpose of the protein (function), and determining how the protein folds (structure). Microfluidic devices are mainly used in the profile and function of proteomics. This analysis usually requires multiple repeating steps and large amounts of costly reagents. Microfluidics would be able to perform these steps quickly with much less reagent [10].

Materials in Use

The numerous materials that can be used to make microfluidic channels include glass, metals, ceramics, and polymers. This report focuses on PDMS because of its ease of processing, flexibility, and transparency; and glass because of its ability to be plasma bonded to PDMS and its ease of use with a laser confocal microscope.

PDMS

PDMS (poly dimethyl siloxane) is a silicon based elastomer (Figure 4) that comes as a base and a curing agent, from its supplier Dow Corning, which are mixed in a 10:1 ratio.

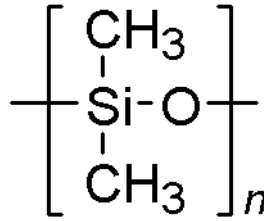


Figure 4 Structure of PDMS [1].

The processing can easily be completed in about 2 hours with a premade mold [11]. The base contains monomer, while the curing agent contains a cross-linker. The base is a viscous liquid, but after cross-linking becomes a hydrophobic flexible solid. Treatments can be done to make the surface temporarily hydrophilic. Plasma oxidizes the surface replacing methyl groups with hydroxyl groups. Plasma can also be used to bond the PDMS surface to another surface like glass or another piece of PDMS, which is useful to make a fourth wall of a microfluidic channel [1].

There are many advantages to using PDMS in microfluidics research. PDMS is inexpensive and easily processed with good resolution. In addition, PDMS creates a strong bond to glass or another PDMS layer with plasma bonding. The thickness of a PDMS layer can be controlled with a spin coating step. PDMS is flexible, so input tubes can be easily integrated into a device. Biocompatibility is also a very desirable property for many research applications [1].

There are also issues with using PDMS in microfluidic systems. Electro-kinetic flow is problematic with PDMS because depositing metals on PDMS is difficult; however, metals can be deposited on glass which is then plasma bonded to the PDMS. In addition, PDMS ages over time, which might change desired

mechanical properties. PDMS also dissolves in many organic solvents which prevents some solvents being used for certain reactions [1].

PDMS processing is very simple (Figure 5). First, a mold is made using soft lithography on SU-8, a common negative photoresist. The base and curing agent is mixed and poured over the mold. Bubbles normally need to be removed using a vacuum chamber. After the PDMS has set, the mold is released and inlet and outlet holes are made in the PDMS. The PDMS is then plasma treated and attached to another surface. Connectors can then be inserted and the device can be used [1].

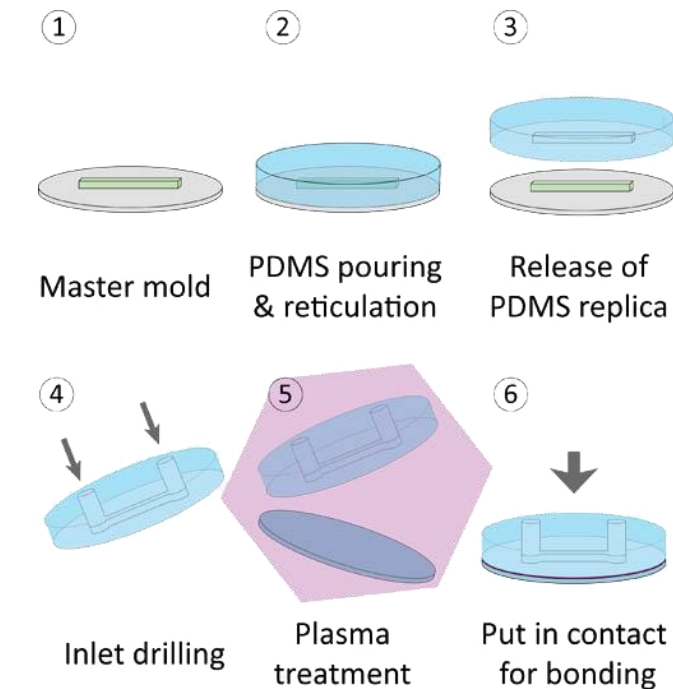


Figure 5 Processing of a PDMS microfluidic chip [1].

Glass

Glass is made of silicon and oxygen arranged in an amorphous structure (Figure 6). Like PDMS, glass can be plasma bonded. The bonding of PDMS to glass is

slightly weaker than the bonding of PDMS to PDMS, which must be considered when determining the pressure within a channel. However, bonding to a slide or cover-slide could make viewing under a microscope easier.

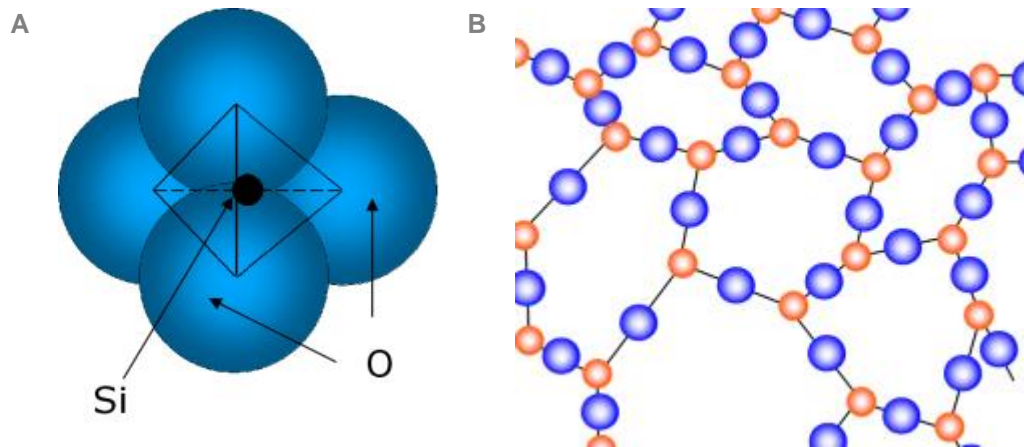


Figure 6 A) Unit cell and B) amorphous structure of glass [12].

Methods of Flow

Determining Type of Flow

On the micro-scale, the type of flow must be considered in the channel. Turbulent flow is what is normally seen on the macro-scale; however, laminar flow is often seen on the micro-scale. Since microfluidics involves making devices on the micro-scale, understanding laminar flow is important. The Reynolds number can show what kind of flow will be present [13]:

$$R_e = \frac{\rho V D}{\mu_d} \quad \text{Equation 1}$$

Where ρ is the density (water = 1g/cm^3), V is the velocity, D is the hydraulic diameter, and μ_d is the dynamic viscosity (water = $1 \cdot 10^{-3} \text{ kg/m} \cdot \text{s}$). For liquids, if the Reynolds number is less than 2000, the fluid is expected to exhibit laminar flow. V can be calculated by:

$$V = \frac{Q}{A} \quad \text{Equation 2}$$

Where Q is the flow rate and A is the cross-sectional area. D , for a rectangular channel, can be calculated by:

$$D = \frac{2ab}{(a + b)} \quad \text{Equation 3}$$

Where a and b are the lengths of the sides. For liquids, laminar flow is present for Reynolds numbers below 2000.

For laminar flow, where mixing depends on diffusion, mixing time can be estimated by:

$$t_{50\%} = \frac{w^2}{D} \quad \text{Equation 4}$$

Where w is the width of the channel and D is the diffusivity (water = $1 \cdot 10^{-9}$ m²/s).

As discussed earlier, micro-mixers are one of the many uses of microfluidics. The time and flow rate are used to determine a mixing length. The above equations estimate the amount of mixing that occurs within a channel of a specified length. This length is used when designing devices.

Although diffusion is a major part of mixing on this scale, other factors also contribute to the degree of mixing, such as velocity profile. How different methods of inducing flow create different types of velocity profiles is discussed in the following sections.

Flow Driven By Capillary Forces

In nature, capillary forces are used to move liquid up small tube-like structures without any additional forces. This process requires the tubes surface to be hydrophilic, unlike PDMS. Adding additional forces can make water flow through a PDMS channel. Capillary pumping applies a temperature gradient across liquid in a channel. The difference in surface tension because of the temperature gradient causes liquid to move through the channel (Figure 7) [14]. A drop will have equal pressure, or surface tension, on both sides and not move, but adding a temperature gradient changes the pressure and allows the liquid to move toward the higher temperature.

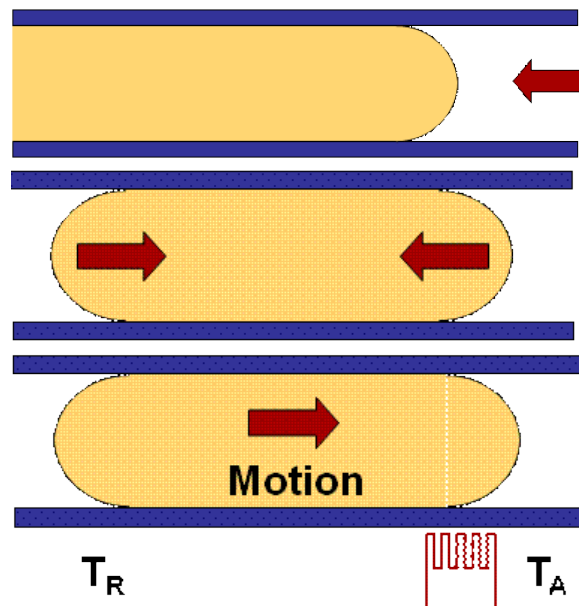


Figure 7 Polar fluid in a hydrophobic channel [14].

Surface tension can be calculated by:

$$\gamma = a - bT$$

Equation 5

Where γ is surface tension, a is 75.83 dyn/cm and b is 0.1477 dyn/cm/°C for water, and T is temperature. As shown in the equation, surface tension is dependent on temperature. Knowing how temperature affects surface tension will allow predictions about the direction of flow.

Pressure Driven Flow

Pressure driven flow is related to the flow rate and fluid resistance by:

$$\Delta P = QR \quad \text{Equation 6}$$

Where ΔP is the change in pressure within the channel, Q is the flow rate, and R is the fluid flow. Fluid flow is calculated by:

$$R = \frac{12\mu_d L}{wh^3} \quad \text{Equation 7}$$

Where μ_d is the dynamic viscosity (water = $1 \cdot 10^{-3}$ kg/m²), and L , w , and h are the dimensions of the channel. The velocity can be calculated by:

$$v = \frac{Q}{A} \quad \text{Equation 8}$$

Where Q is the flow rate and A is the cross-sectional area of the channel. Often a syringe pump is used to apply a specific flow rate.

The pressure needs to be low enough to not break the bonding of the PDMS to the glass cover slide or leak at the input and output holes. The velocity of the fluid must be within a range so that a single particle within the fluid remains within the frame of view of the microscope. More detail about the microscope is described in Section VII. In addition, pressure within the channel and the fluid's velocity increases with increasing applied flow rate.

Pressure driven flow is known for a parabolic profile when moving liquid through the channel. This means that the fluid flows at different rates near the wall of the channel and at the middle.

Electro-Kinetic Forces

Although there are many different types of electro-kinetic phenomena, four main types are of interest (Table I). These forces differ in whether a force or an electric field is applied and whether that application causes a solid or liquid to move.

Table I Comparison chart of four main types of electro-kinetics.

| | Stationary Solid | Stationary Liquid |
|----------------------|---------------------|-------------------------|
| Apply Force | Streaming Potential | Sedimentation Potential |
| Apply Electric Field | Electro-Osmosis | Electrophoresis |

Streaming Potential

Streaming potential occurs when an electric field is created by the movement of a polar liquid. This happens with pressure driven flow through a channel. The created potential can be calculated by:

$$V = \frac{\zeta \epsilon_0 \epsilon_r \Delta P}{\eta \kappa} \quad \text{Equation 9}$$

Where ζ is the zeta potential of the wall and liquid interface, ϵ_0 is the permittivity of free space (8.85×10^{-21} As/Vm), ϵ_r is the relative permittivity for PDMS, ΔP is the applied pressure, η is the viscosity and κ is the solution's conductivity [15].

Streaming potential also has a parabolic profile due to the difference in ion concentrations near the wall and at the middle of the channel (Figure 8).

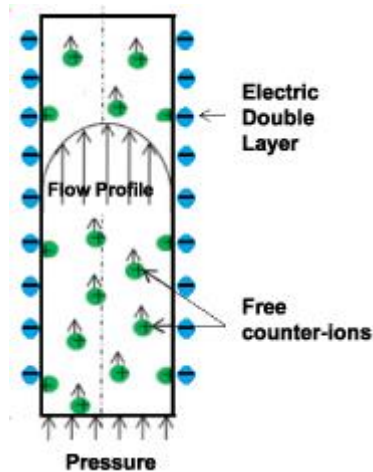


Figure 8 Streaming potential in a channel [16].

Sedimentary Potential

Sedimentary potential occurs when an electric field is created by the movement of particles, often particles settling in a liquid. The created potential can be calculated by:

$$V = \frac{\zeta \epsilon_0 \epsilon_r (\rho - \rho_o) g}{\eta \kappa} \quad \text{Equation 10}$$

Where ζ is the zeta potential of the wall and liquid interface, ϵ_o is the permittivity of free space (8.85×10^{-21} As/Vm), ϵ_r is the relative permittivity for PDMS, ρ is the density of the solution, ρ_o is the density of the solvent, g is the force of gravity (9.81 m/s^2), η is the viscosity and κ is the solution's conductivity [15]. Streaming and sedimentary potential can occur together and counteract each other.

Electrophoresis

Electrophoresis occurs when particles move due to an applied voltage. The velocity of the particles can be calculated by

If the Debye length, a measure of electrostatic affect in a solution, is small compared to the particle radius:

$$v = \frac{\epsilon_0 \epsilon_r \zeta \vec{E}}{\eta} \quad \text{Equation 11}$$

If the Debye length is large compared to the particle radius,

$$v = \frac{2}{3} \frac{\epsilon_0 \epsilon_r \zeta \vec{E}}{\eta} \quad \text{Equation 12}$$

Where ϵ_0 is the permittivity of free space (8.85×10^{-21} As/Vm), ϵ_r is the relative permittivity for PDMS, ζ is the zeta potential for the wall liquid interface, \vec{E} is the applied electric field, and η is the viscosity [15].

Electro-Osmosis

Electro-osmosis occurs when fluid moves due to an applied voltage (Figure 9).

The velocity of the fluid can be calculated by:

$$v = \frac{-\epsilon_0 \epsilon_r \zeta \vec{E}}{\eta} \quad \text{Equation 13}$$

Where ϵ_0 is the permittivity of free space (8.85×10^{-21} As/Vm), ϵ_r is the relative permittivity for PDMS, ζ is the zeta potential for the wall liquid interface, \vec{E} is the applied electric field, and η is the viscosity. Electro-osmosis has a plug-like profile, making more uniformity across the channel. A uniform profile is ideal in mixing systems, creating a more uniform mix more quickly.

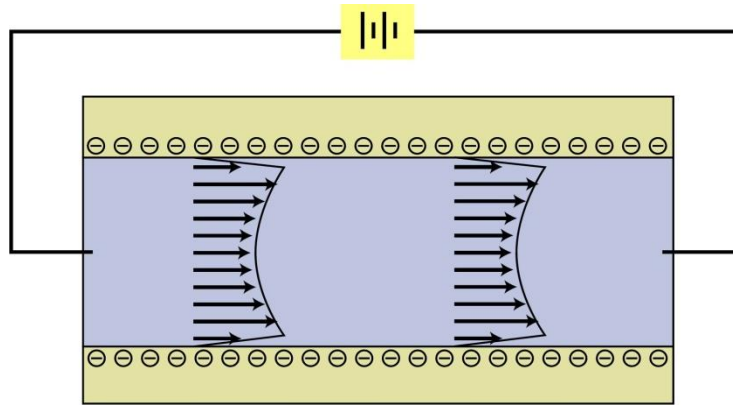


Figure 9 Electro-osmotic flow in a channel [17].

Since fluid cannot be seen flowing under a microscope, particles are often added. If the particles have a surface charge, they are acted on by electrophoresis in addition to the pressure of electro-osmosis from the fluid. This could cause different results than expected [15]. Electro-osmosis is the goal when applying an electric field on a microfluidic chip; however, if the particles in the fluid have a surface charge, then an electrophoretic force also acts on them. Overall, the sum of the electro-osmotic and electrophoretic forces is measured.

Measuring Velocity

Knowing the velocity of liquid within a channel is important when designing microfluidic devices so that the correct type of flow is used for the specific application. The different ways to measure fluid velocity using flowmeters include:

- Differential Pressure Flowmeters
- Velocity Flowmeters
- Positive Displacement Flowmeters
- Mass Flowmeters
- Open Channel Flowmeters [18]

However, these flowmeters are meant to be used on the macro-scale and are not sensitive enough for the micro-scale.

For micro-fluidics other flow measurement techniques are used such as laser Doppler velocimetry, molecular tagging velocimetry, and particle image velocimetry [3].

Laser Doppler Velocimetry (LDV)

Like the Doppler effect that is heard with moving objects, this method uses the Doppler effect with light. Particles are added to a fluid that scatters a particular wavelength of light. A monochromatic laser is used to provide the light source which is then detected by a photomultiplier tube (PMT). The difference in wavelengths can then be used to determine the speed of the particles in the fluid (Figure 10). This type of measurement does not require be in contact with the channel and can get measurements quickly, but required the channel to be made of transparent materials, have varying accuracy, and are expensive [19].

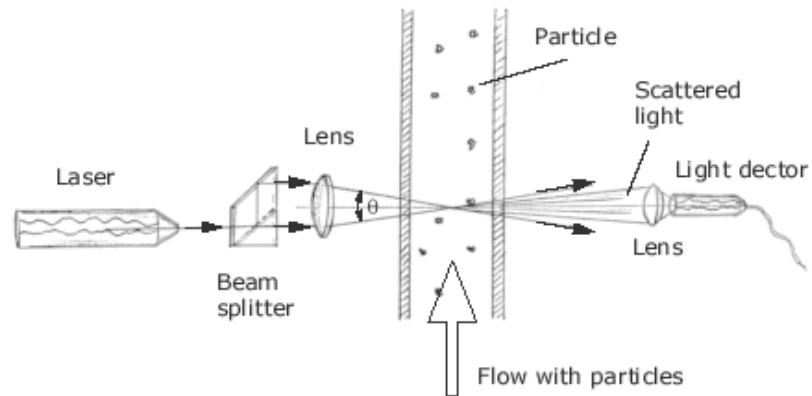


Figure 10 Set-up of a laser Doppler velocimeter [19].

Molecular Tagging Velocimetry (MTV)

For MTV, fluorescent or phosphorescent molecules are added to a fluid. A light source is used to excite the molecules, normally in a pattern like a grid. These are imaged multiple times in a short time interval and then processed to create velocity measurements [20].

Particle Image Velocimetry (PIV)

Like MTV, PIV uses fluorescence to see fluid flow. Fluorescent particles are added to the fluid and images are taken in short time intervals. These are then processed to create velocity measurements [3].

In this case, fluorescent polystyrene (PS) particles are used. PS particles of a specific size or molecular weight are easy to manufacture since the polymerization process is easily controlled. Fluorescent molecules can be attached to these polymer particles. Fluorescence is the absorption of high energy light and then emitting lower energy light.

A laser confocal microscope can be used to view these particles (Figure 11) [21]. This microscope can change the light used to view only the fluorescent particles. In addition, the microscope uses a dichromatic mirror to only see emitted light and not reflected excitation light. Also optical lenses are used to separate the focal point of different colors of light. A pinhole can be put at this focal point to filter out the undesirable colors. A laser is used as the excitation light. There is a small depth of field on this type of microscope, so only a certain plane in the sample is seen at one time.

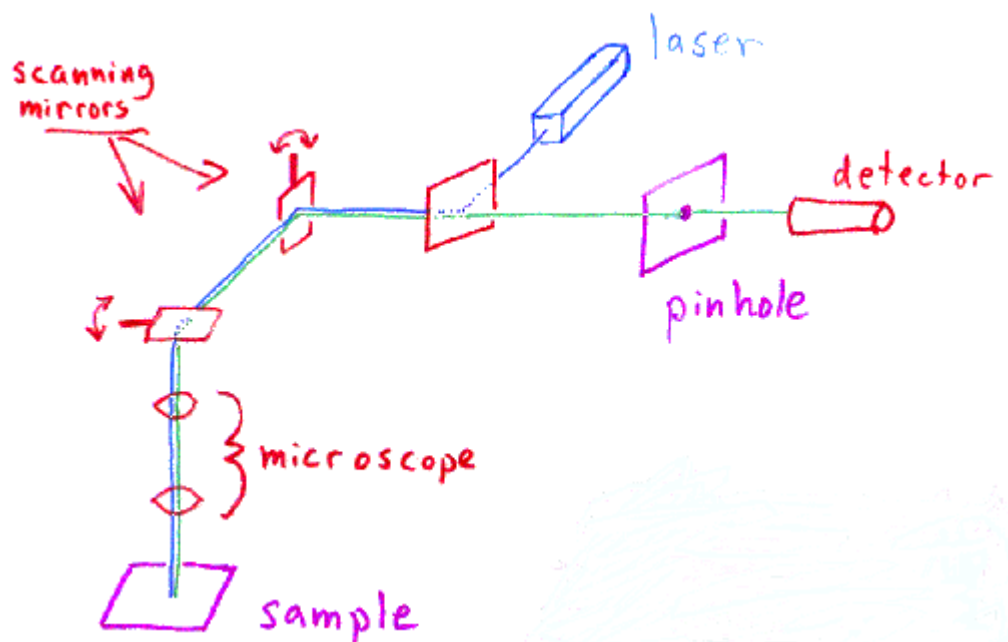


Figure 11 Schematic of components of a laser confocal microscope [21].

Societal Impact

The field of microfluidics contributes to society in many positive ways. In the medical field, microfluidics is used to supply a steadier concentration of medication to patients to eliminate dangerous spikes and valleys. This is

especially helpful for insulin and blood pressure medicines. Microfluidic devices allow medication to be administered even when trained personnel are not available, broadening the ability to improve health world-wide. In addition, there are environmental benefits. Waste from medical research and products such as needles is extensive. Microfluidics uses less material, creating less waste, and, therefore, reducing the amount trash headed to our landfills [22].

Project Definition/Research Question

Compare electro-kinetic and pressure driven flow rates and velocity profiles (near wall vs. middle) in a microfluidic chip made of PDMS and/or glass using particle imaging velocimetry (PIV) of an aqueous solution of fluorescent polystyrene (PS) particles on a laser confocal microscope (LCM).

The expectation is that flow rates will have different ranges between the two methods because of allowed pressure within a channel without leaking. The electro-kinetic system will have a more uniform velocity profile allowing more even and quicker mixing, being better for mixing applications.

Previous research at Cal Poly has involved pressure-driven flow. This research will attempt to determine a method for creating electro-kinetic driven flow in Cal Poly labs. Both these flow techniques will be measured for comparison.

Experimental Procedures

A mask used for a previous senior project was used to create the pressure-driven channels. While testing this channel, parameters for the laser confocal microscope were observed. A new mask was fabricated in AutoCAD for the electro-kinetic channels with these parameters (Figure 12).

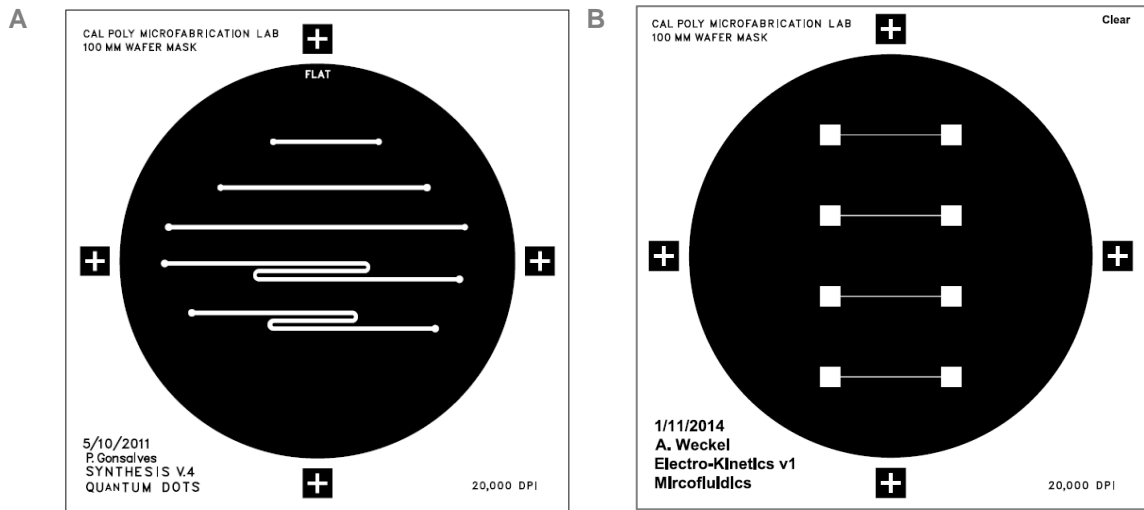


Figure 12 A) Mask used for fabrication of pressure-driven channels. The top channel was used with dimensions of 1mm wide and 25mm long. B) Mask designed in AutoCAD for fabrication of electro-kinetic channels. Channel dimensions are 170 μ m wide and 25mm long. The wells are 5mm squares

Fabrication Procedure

Microfluidic channels were made using soft lithography processing methods (Figure 13). A more detailed procedure can be found in Appendix A.

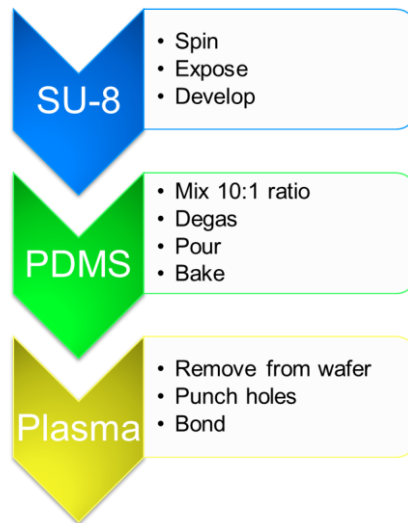


Figure 13 Process flow chart for the fabrication of PDMS channels.

SU-8

A mold was made using SU-8 on a silicon wafer. The SU-8 was spun so that the pressure driven channels were 180um deep and the electro-kinetic channels were 45um deep.

PDMS

Because the microscope is inverted, about 100mL of PDMS mixture was poured over the wafers to create a thick channel to give some support. One hole was punched at each end for the pressure-driven channel and two holes were punched for the electro-kinetic channel, one for the tubing and one for the wire.

Plasma Bonding

First, the individual channels were cut out and a cover-slide was cleaned. They were placed on an acrylic surface and coated with plasma about 5 times and

then quickly placed together. Pressure was carefully added around the channel without putting pressure on the channel to avoid bonding within the channel.

At first the PDMS channels were directly bonded to a glass cover-slide. This caused some issues during testing with many particles sticking to the walls which made following a particle across the channel difficult. For the final channels, a thin layer of PDMS was spun on the cover-slide prior to plasma bonding. This helped a little with reducing the amount of particles sticking, but very few particles seemed to be moving. Using the same diluted solution on the sticking channels may have caused the solution to be diluted further, so the dilution was remixed from the original particle solution.

Testing Procedure

Microscope Parameters

Twenty mil inner diameter tubing was used to insert fluid into the channel.

Images were taken at 10x magnification. The images were 256 pixels square.

Each pixel was taken 2 μ s apart going across and down the image. The pixel size was 4.971 μ m square.

The channel was set up on the laser confocal microscope, which is an inverted microscope. Fluid was pumped throughout the channel and tubing. This fluid was then allowed to come to rest which normally took about 30 minutes.

Pressure-Driven Flow Setup

For pressure-driven flow, a New Era Pump Systems syringe pump was used (Figure 14). A 1mL syringe pump was used rather than a 3mL syringe pump with an inner diameter of 4.69mm. These syringe pumps have a tendency to pulse at lower flow rates, which may cause inconsistent measurements.

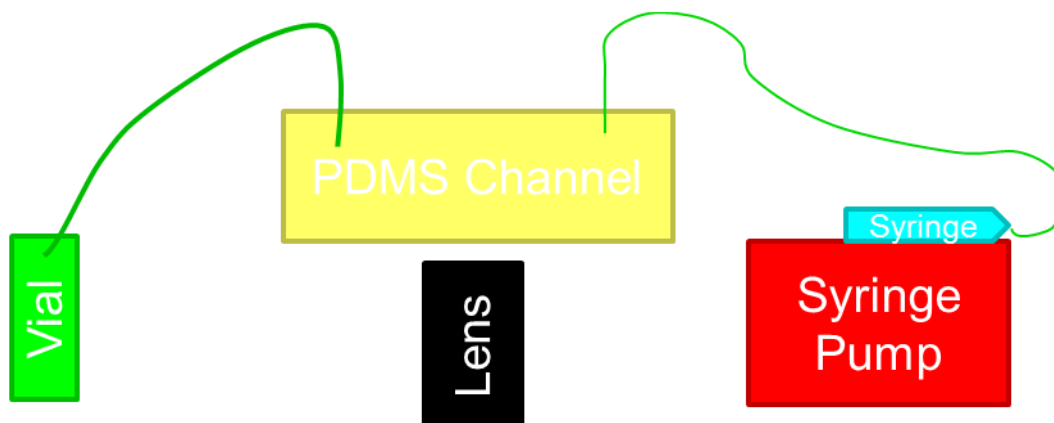


Figure 14 Setup of pressure-driven flow channel.

For pressure-driven flow a pump rate was set on the syringe pump and allowed to pump for 10minutes before images were taken.

Electro-Kinetic Flow Setup

Multiple methods were used to obtain data for electro-kinetic flow, but none seemed consistently good (Figure 15). At first, a voltage was applied across the channel, which had varied results. The particles would flow in one direction for a while and then switch directions. Some force build up was hypothesized to be causing this switch. A small flow rate was applied as a base in addition to the applied voltage to try to remove the effects of the force build up, but the flow rate seemed to overpower the voltage.

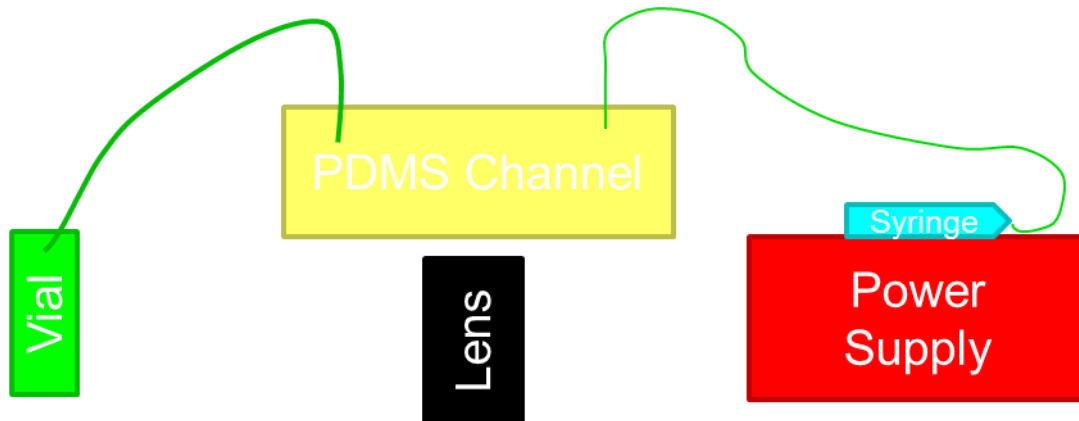


Figure 15 Setup of electro-kinetic flow channel.

Many difficulties were found during testing. Measurements were gotten that are close to the calculated value, much higher, and much lower. Air bubbles in the system interfered with the particle movement, causing very strange numbers. Saline solutions had more surface properties which is very influential for the electro-kinetics, but after a while the particles would stop moving.

Results and Analysis

The images were taken at one plane in the channel at multiple times. The microscope was set to take multi-tiff images in stacks of 50. Sub-stacks were made and overlaid in different colors using Image-J software. Originally, only 2 images were used for the overlay, but measurements might not be the same particle at two different times but two different particles going in and out of the plane of view. To fix this problem, 8 images were overlaid, to create a colored line to be more certain that measurements were taken from the same particle at different times instead of different particles moving in and out of the plane (Figure 16).

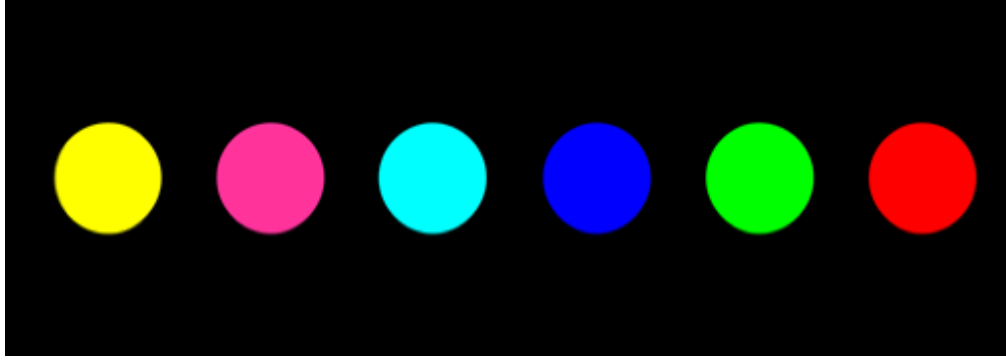


Figure 16 Example overlay of 8 images in different colors to allow for PIV measurements.

The x and y pixel location and the x, y, and z color values for these moving particles were recorded and analyzed in Excel. The color values were used to match the particle with one of the 8 images. This determined the time at which the particle was in that position (Figure 17). In addition, a line was fit to model the wall, so a velocity profile could be created to determine how far the particle was from the wall.

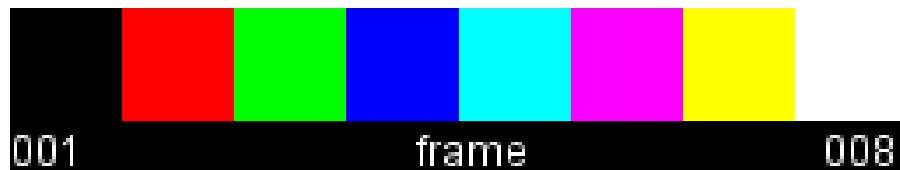


Figure 17 Time-lapse color coder used to analyze stacks of 8 images that had been overlaid in different colors.

Pressure-Driven Results

Results were analyzed for 0.5 and 0.75 $\mu\text{L}/\text{min}$ (Figure 18). Using JMP statistical software, data indicated no significant velocity difference between different regions along the channel, so the parabolic velocity profile is not present. JMP output can be found in Appendix B. The dimensions of the channel, being wide and flat, caused the parabolic profile to only be apparent very near the wall of the

channel. However, this area had many sticking particles so this was not verifiable.

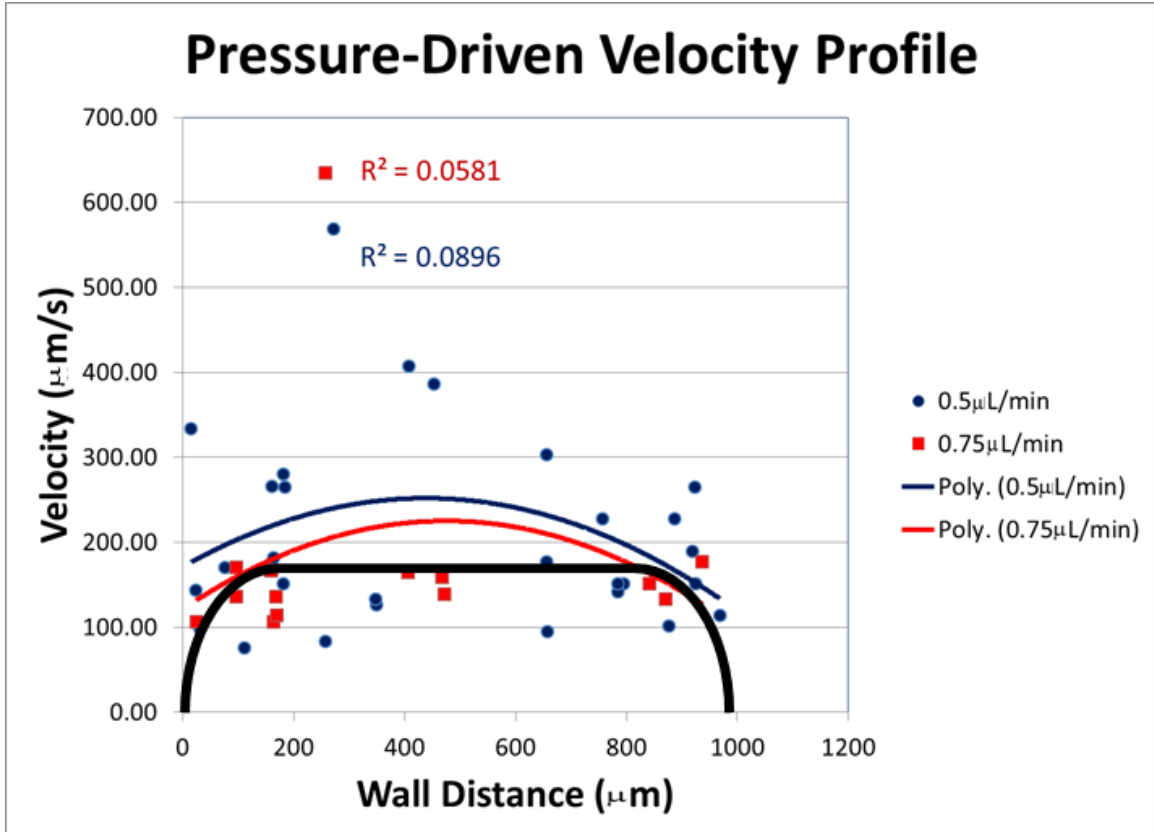


Figure 18 Pressure-driven results for 0.5µL/min (blue) and 0.75µL/min (red). For a wide and flat channel the parabolic profile would only be apparent near the wall of the channel (black).

The overall average velocities conflict with logic (Table II). The 0.75uL/min average is less than the 0.5uL/min average. Inaccuracies in the syringe pump were hypothesized to be the cause. In addition, there is lots of variation in the data. This is probably from wall interactions since the depth of the particle cannot be determined when imaging. Finally, the calculated velocities are different from the expected velocities. This was also possibly from inaccuracies in the syringe pump.

Table II Pressure-driven results summary.

| Pump Rate (uL/min) | Average Velocity (um/s) | Standard Deviation | Expected Velocity (um/s) |
|--------------------|-------------------------|--------------------|--------------------------|
| 0.5 | 205.83 | 112.92 | 46.3 |
| 0.75 | 178.16 | 133.30 | 69.44 |

Syringe Pump Verification

Since the pressure driven results were consistently higher than expected the syringe pump was suspected to not be accurate for low flow rates. Using a Denver Instruments analytical scale, measurements were taken every 5 minutes for 90 minutes (Figure 19).

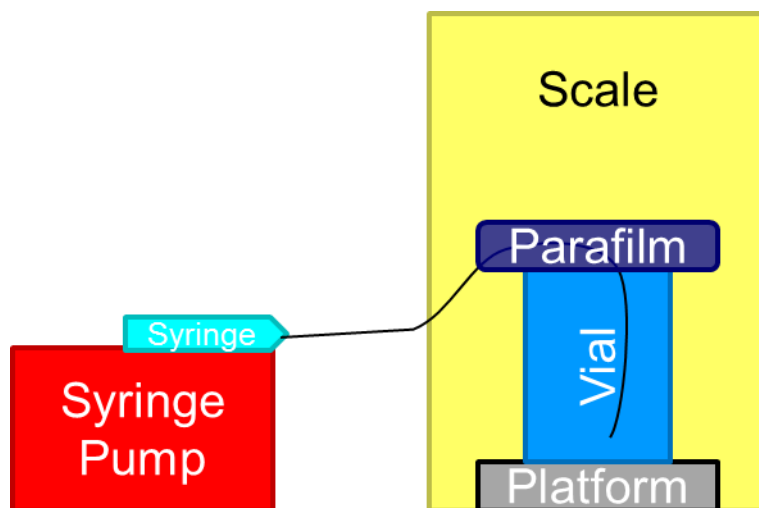


Figure 19 Setup for syringe pump verification.

This data was graphed in Excel and fit with a linear regression line (Figure 20). The slopes showed the true flow rate for the syringe pump setting. The flow rates were actually a little lower than the setting which makes the data make even less sense. There could possibly still be some pulsing in the syringe pump which

might explain some of the inconsistencies seen but not show in the overall flow rate.

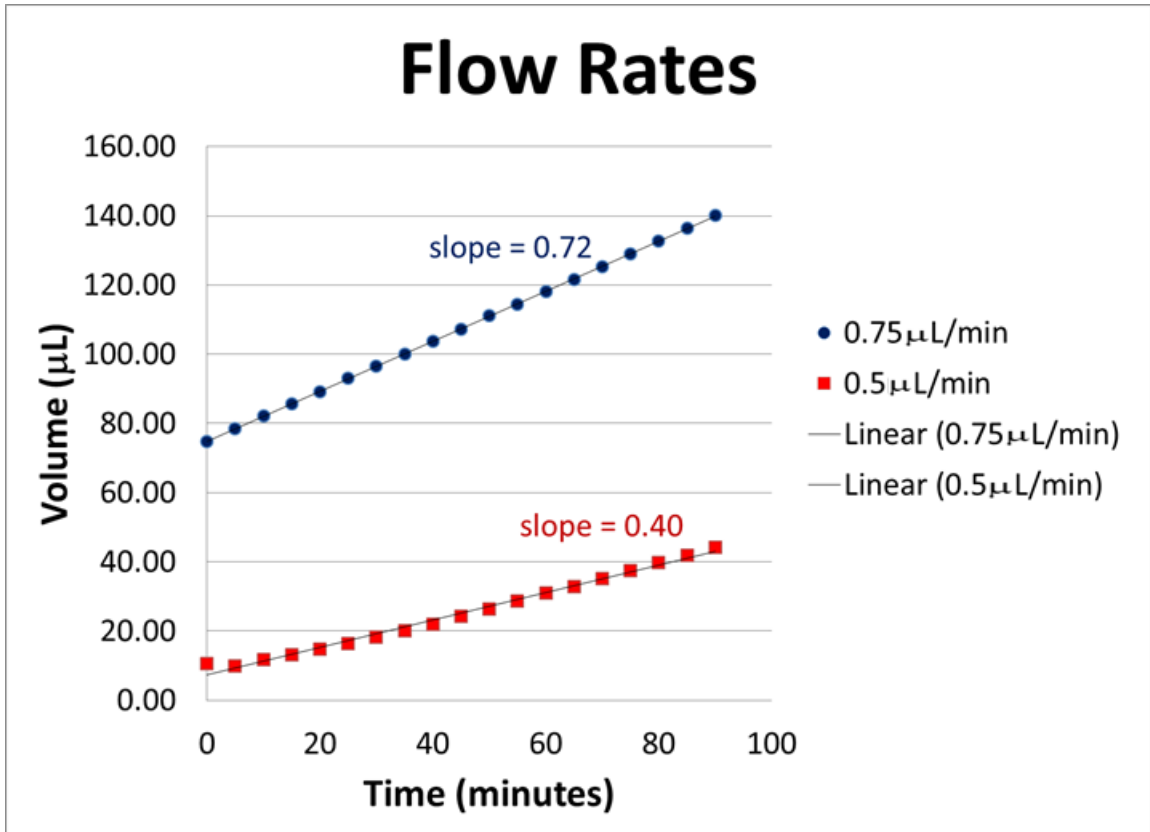


Figure 20 Results of syringe pump verification.

Electro-Kinetic Results

There were many issues with the electro-kinetic flow, and none of the obtained measurements were reliable. Often flow would switch directions at random intervals. Charge build up was thought to be causing directions to change. Pressure was added as a base to try to remove this buildup within the channel and get a more consistent flow. Bubbles also appeared easily when testing electro-kinetic flow, especially when adding pressure to remove the reverse flow direction (Figure 21). This also happened with pressure-driven flow but not as

often. The parabolic velocity profile associated with pressure-driven flow is very apparent with the bubble. The bubble was also very good at clearing out the florescent particles from the channel, even many of the ones that were stuck.

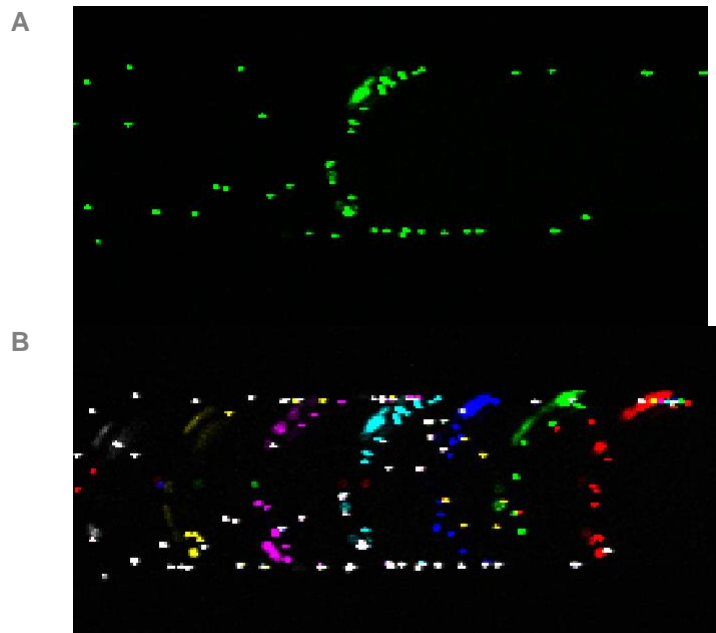


Figure 21 Bubble traveling through the channel with $0.25\mu\text{L}/\text{min}$ of pressure and 50V. The voltage appears to have no impact on the flow.

Research showed that bubbles are often introduced in microfluidics from connecting tubing or moving the channel. In addition changes in temperature, pressure, surface properties of the channel, and properties of the fluid within the channel can cause bubbles to grow. A simple bubble trap can be created at the inlet where bubbles can flow out of the way of the channel. This provides temporary help since the bubble is not completely removed from the system. However, the length of time depends on the flow rates and the size of the bubble trap [23].

Conclusions & Recommendations

In conclusion, the fabrication process worked well and can be used for a variety of channels. Pressure driven flow in this channel will not show a parabolic profile since the width to height ratio is large. In addition, there is variation between the particles and the data is different from expected. Electro-kinetic driven flow is greatly influenced by air bubbles in the system and surface interactions. Finally, the laser confocal microscope did work as a way to perform PIV on microfluidic chips.

This research will be continued as my master's thesis next year. The following changes will be made to narrow down the variability in the measurements. First, deeper channels to make the cross-section more square will help get a measurement without having particles interact with the wall. Surface properties are greatly influential on this scale and could be causing some of the variability seen. In addition, a squarer channel will allow the parabolic flow profile to be identified. Second, a glass channel will also influence the surface properties. Glass has very different surface properties than PDMS and is less gas permeable, which might help with the bubble problem. Third, particles that fluoresce at different wavelengths would help in tracking the particle through the channel, making identification that a pixel is the same particle at different times instead of two particles going in and out of the plane of view easier.

Acknowledgments

This research would not have been possible without the support of:



Dr. Harding for being my senior project advisor and giving me ideas on my project.



Dr. Savage for being my thesis advisor and giving me a project topic and encouragement throughout the project.



Dr. Laiho for showing me how to use the laser confocal microscope and helping me when the software update caused issues.



Professor Mayer for giving me suggestions on fabrication and testing.



Dr. Clague for giving me suggestions for things to try next year and especially letting me pet his dog.



Nash Anderson for his previous work on this project at Cal Poly.

References

- [1] G. V. Casquillas, "Tutorials," Elveflow, [Online]. Available: <http://www.elveflow.com/>. [Accessed 27 November 2013].
- [2] R. Savage, "MEMS Design, Cantilever, Accelerometer," in *MATE 430*, San Luis Obispo, 2013.
- [3] N.-T. Nguyen and S. T. Wereley, *Fundamentals and Applications of Microfluidics*, Norwood: Artech House, Inc., 2002.
- [4] H.-S. Chuang, "Microfluidics for Life Science and Chemistry Microfilters & Microseparators," in *Fundamentals, Characterizations and Applications of Microscale Fluids*, 2012.
- [5] H.-S. Chuang, "Microfluidics for Life Science and Chemistry: Microneedles & MicroMixers," in *Fundamentals, Characterization and Applications of Microscale Fluids*, 2012.
- [6] University of Notre Dame, "From the Director," Center for Microfluidics and Medical Diagnostics, 2004. [Online]. Available: <http://microfluidics.nd.edu/about/>. [Accessed 27 November 2013].
- [7] T. Srinivasan, "Microfluidics for DNA Analysis," in *EE C 245/*.
- [8] R. C. Lo, "Application of Microfluidics in Chemical Engineering," *Chemical Engineering & Process Techniques*, vol. 1, no. 1002, pp. 1-3, 2013.
- [9] L. Kang, B. G. Chung, R. Langer and A. Khademhosseini, "Microfluidics for drug discovery and development: From target selection to production lifecycle management," *Drug Discovery Today*, vol. 13, pp. 2-13, 2008.
- [10] E. M. Miller, S. Freire and A. R. Wheeler, "Proteomics in Microfluidic Devices," pp. 1749-1758.
- [11] Dow Corning, "SYLGARD® 184 SILICONE ELASTOMER KIT," Dow Corning Corporation, 2013. [Online]. Available: <http://www.dowcorning.com/applications/search/default.aspx?r=131en>. [Accessed 28 November 2013].
- [12] S. o. M. s. a. Engineering, "Ceramics," The University of New South Wales, [Online]. Available: <http://www.hsctut.materials.unsw.edu.au/Ceramics/ceramics1a.htm>. [Accessed 4 June 2014].
- [13] R. Savage, *Writer, MATE 225 Microfluidic Project*. [Performance]. 2012.
- [14] T. A&M, "ALChemE: Active Learning in Chemical Engineering," Chemical Engineering Department Online Curriculum Reform Project, [Online]. Available: http://alcheme.tamu.edu/?page_id=1088. [Accessed 28 November 2013].
- [15] G. K. Butt, *Physics and Chemistry of Interfaces*, Weinheim: Wiley, 2006.
- [16] B. K. a. L. M. Weiland, "Experimental investigation of the streaming potential hypothesis for ionic polymer transducers in sensing," *IOP science*, vol. 22, no. 3, 2013.
- [17] D. J. Laser, "Electrokinetics and Electroosmotic Flow," Design Division, Department of Mechanical Engineering, Stanford University, [Online]. Available: http://micromachine.stanford.edu/~dlaser/research_pages/electrokinetics_and_eof.html.

[Accessed 28 November 2013].

- [18] The Engineering Toolbox, "Types of Fluid Flowmeters," The Engineering Toolbox, [Online]. Available: http://www.engineeringtoolbox.com/flow-meters-d_493.html. [Accessed 28 November 2013].
- [19] Velocimetry, "Principles," Velocimetry Technology (P) Limited, [Online]. Available: <http://velocimetry.net/principle.htm>. [Accessed 1 June 2014].
- [20] Michigan State University, "Molecular Tagging Velocimetry (MTV)," College of Engineering, [Online]. Available: <http://www.egr.msu.edu/tmual/MTV.html>. [Accessed 1 June 2014].
- [21] "How does a confocal microscope work?," [Online]. Available: <http://www.physics.emory.edu/~weeks/confocal/>. [Accessed 28 November 2013].
- [22] N. Anderson, "Bond Strength Characterization of SU-8 to SU-8 for Fabricating Microchannels of an Electrokinetic Microfluidic Pump," California Polytechnic State University, San Luis Obispo, 2012.
- [23] W. Zheng, Z. Wang, W. Zhang and X. Jiang, "A simple PDMS-based microfluidic channel design that removes bubbles for long-term on-chip culture of mammalian cells," *Lab Chip*, pp. 2906-2910, 2010.
- [24] H. Mayer, "BMED 435 Microfabrication Processing: Microfluidic Mixer Process Sequence," California Polytechnic State University, San Luis Obispo, 2014.
- [25] H. Mayer, "Soft Lithography-Microfluidics Lab Manual," California Polytechnic State University, San Luis Obispo, 2007.

Appendices

A. Fabrication Procedure

Cleaning

Piranha Clean

- Mix 9:1 ratio of $\text{H}_2\text{SO}_4:\text{H}_2\text{O}_2$ in large beaker
- Heat to 70°C (takes about 30 minutes on hot plate), check temperature with thermometer
- Submerge for 10 minutes at 70°C
- Tilt and shake when removing to drip as little as possible
- Quench rinse in DI water 4 times

Remove Native Oxide

- Submerge to 30 seconds in BOE (buffered oxide etchant) at room temperature
- Quench rinse in DI water 4 times

Spin Rinse and Dry

- Put through one cycle of the SRD

Dehydrate Bake

- Place wafer on hot plate at 150°C for 10 minutes to remove solvents that could inhibit adhesion in next steps



SU-8 Processing

Spin Coat

- Remove SU-8 2050 from fridge 24 hours before using

- Prepare spin coater by lining with aluminum foil and place wafer
- Pressure Driven Spin Recipe
 - Pour about half-dollar sized amount of resist on wafer
 - Spread at 500rpm with 100rpm/s acceleration for 1 minute
 - Level at 1500rpm with 300rpm/s acceleration for 3 minutes
- Electro-Kinetic Spin Recipe
 - Pour about 2-3mL of primer on center of wafer
 - Spread at 300rpm for 30 seconds
 - Level at 3000rpm for 20 seconds
 - Pour about half-dollar sized amount of resist on wafer
 - Spread at 400rpm for 20 seconds
 - Level at 3000rpm for 35 seconds
 - Decelerate at 300rpm for 5 seconds

Remove Edge Bead

- On top take razor along edge of wafer to remove resist
- On bottom take clean room towel with acetone and wipe

Soft Bake

- 60°C for 10 minutes on hot plate
- 85°C for 10 minutes on hot plate
- Cool on towel on counter



Expose

- Use aligner 1 in Cal Poly's clean room with a light integral of 34
- Use Omega filter to remove wavelengths below

350nm and prevent v-shaped walls



Post Exposure Bake

- 60°C for 10 minutes on hot plate
- 85°C for 10 minutes on hot plate
- Cool on towel on counter

Develop

- Submerge in PGMEA (polypropylene glycol methyl ether acetone) developer for 9 minutes
- Rinse with IPA
- If white film forms, develop for 30 seconds more

Clean

- Place in SRD for 1 cycle

Hard bake

- 150°C for 10 minutes on hot plate



SU-8 Resist Thickness Graph

Spin speeds can be changed to achieve specific film thicknesses for SU-8 (Figure 22).

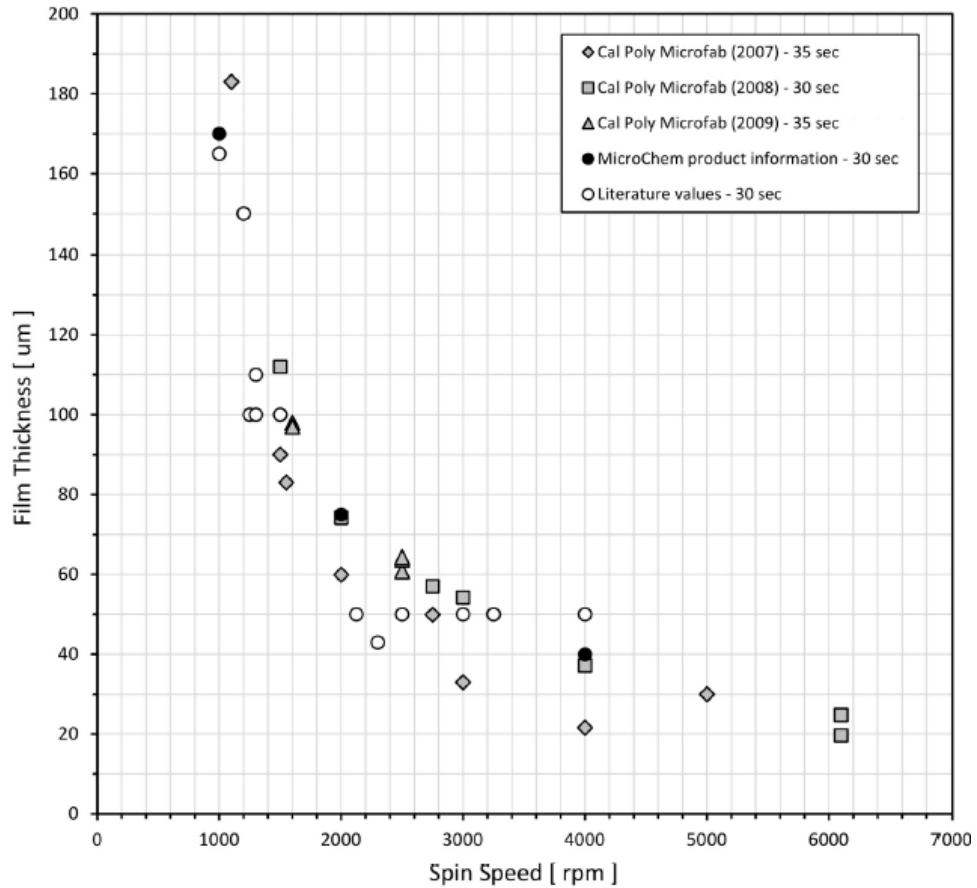


Figure 22 This graph shows how spin speed related to film thickness of SU-8 2050 at Cal Poly in the past. This can be used to determine spinning parameters to obtain required thicknesses of SU-8 [24].

PDMS Processing

Mix

- Add 90mL of base to stirring cup
- Add 9mL of curing agent to cup
- Mix thoroughly

De-gas

- Place cup in vacuum chamber and seal chamber
- Apply vacuum as needed until bubbles are removed

Prepare Petri Dish

- Line petri dish with aluminum foil
- Place wafer at bottom of petri dish

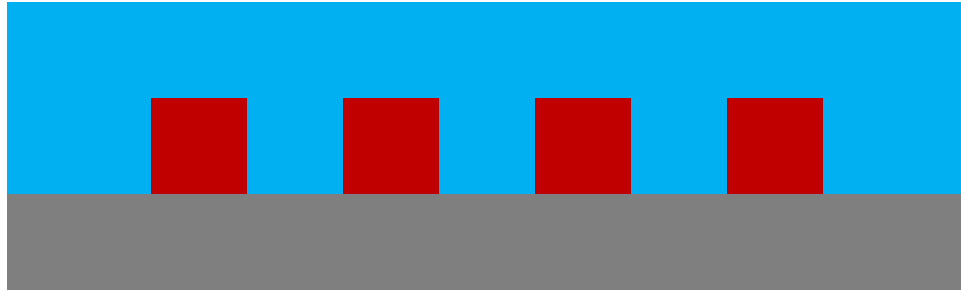
Pour

- Pour PDMS mixture over wafer careful to not add bubbles

- De-gas again if necessary
- Make sure wafer does not lift from bottom of petri dish

Cure

- Place in oven at 70°C for 2 hours



Final Assembly

Prepare Channel

- Use razor blade to cut out individual channels
- Peel channel from wafer
- Punch holes using hole punch kit with 16 gauge needle
- Make sure needle tips are sharp
- Punch one hole for pressure-driven channels and two holes for electro-kinetically driven channels



Prepare Cover-Slide

- Mix 10mL of base with 1mL curing agent and degas
- Prepare spin coater by lining with aluminum foil
- Use special connection for cover-slides
 - Cover exposed areas with tape for easy cleaning

- Pour dime-sized amount of PDMS
- Spin recipe
 - Spread at 500rpm for 20 seconds
 - Level at 3500rpm for 150 seconds
- Cure in petri dish in oven at 70°C for 1 hour



Plasma Bond

- Clean surfaces with masking tape
- Place on acrylic surface and coat 3-5 times with argon plasma
- Place together and apply pressure around channel but not on channel to prevent bonding within channel
- Place in oven at 70°C for 20 minutes



PDMS Thickness Graph

Film thicknesses of PDMS can be changed by changing spin speed or spin time (Figure 23). Film uniformity is greatly affected by dust particles on the surface.

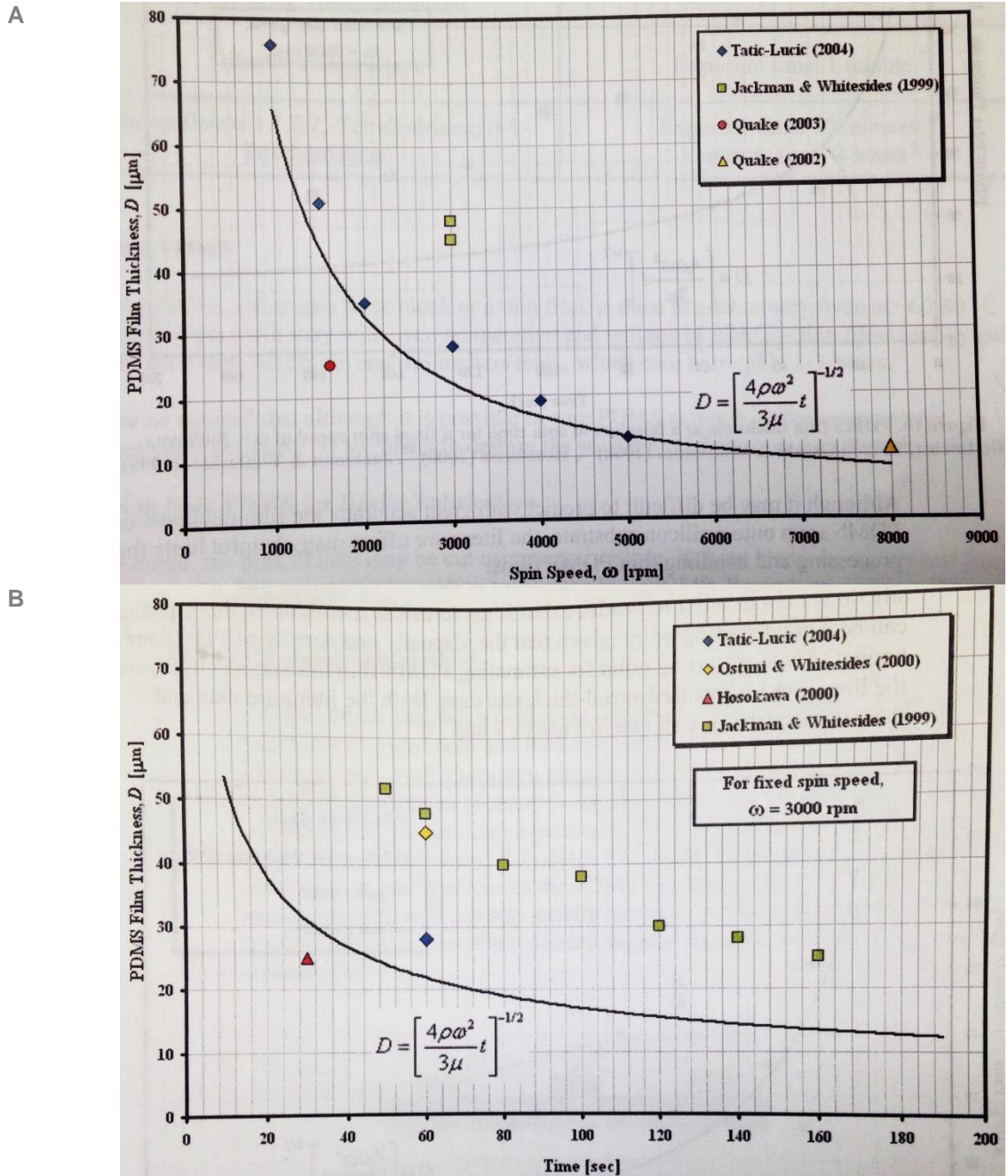


Figure 23 These graphs can be used to determine spinning parameters for PDMS on the cover-slide. A) Different PDMS spin speeds for a 60 second spin. B) Different PDMS spin times for a 3000rpm spin speed [25].

B. JMP Output for Pressure-Driven Data

A t-test was run to determine if the center of the channel had particles with higher velocity than the edge. The edge region was taken as the 300 μm closest to the

edge on each side of the channel when viewed from the microscope. For 0.5 μ L/min, the t-ratio was found to be -0.71 with a probability of 0.24 (Figure 24). For 0.75 μ L/min, the t-ratio was found to be 0.34 with a probability of 0.63 (Figure 25). For 95% confidence, these results show no difference between the velocities found at the center and edge of the channel.

0.5 μ L/min

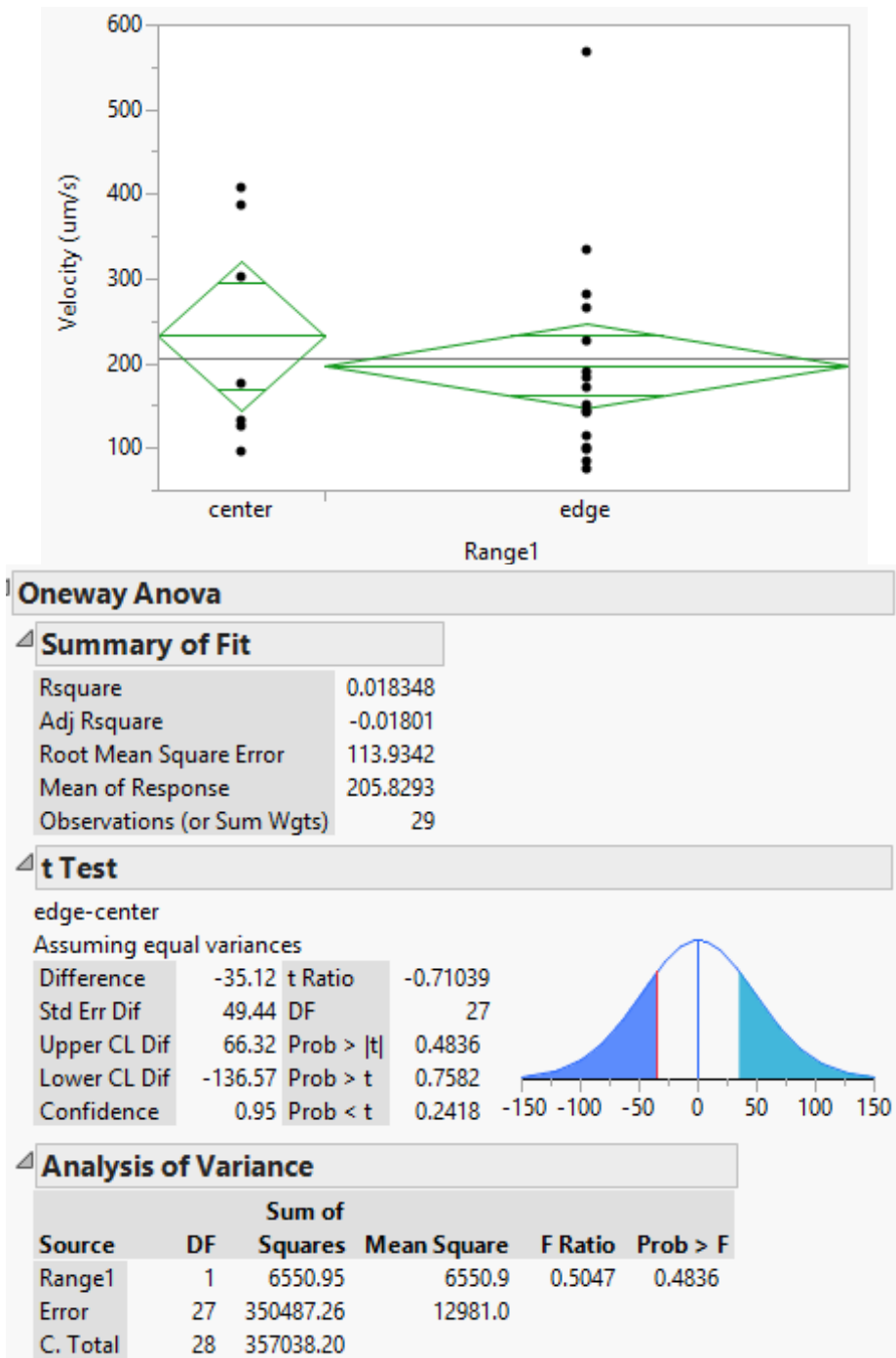


Figure 24 JMP output for 0.5 μ L/min of flow pressure. The edge is within 300 μ m of the wall. There is no significant difference between the regions of the channel.

0.75 μ L/min

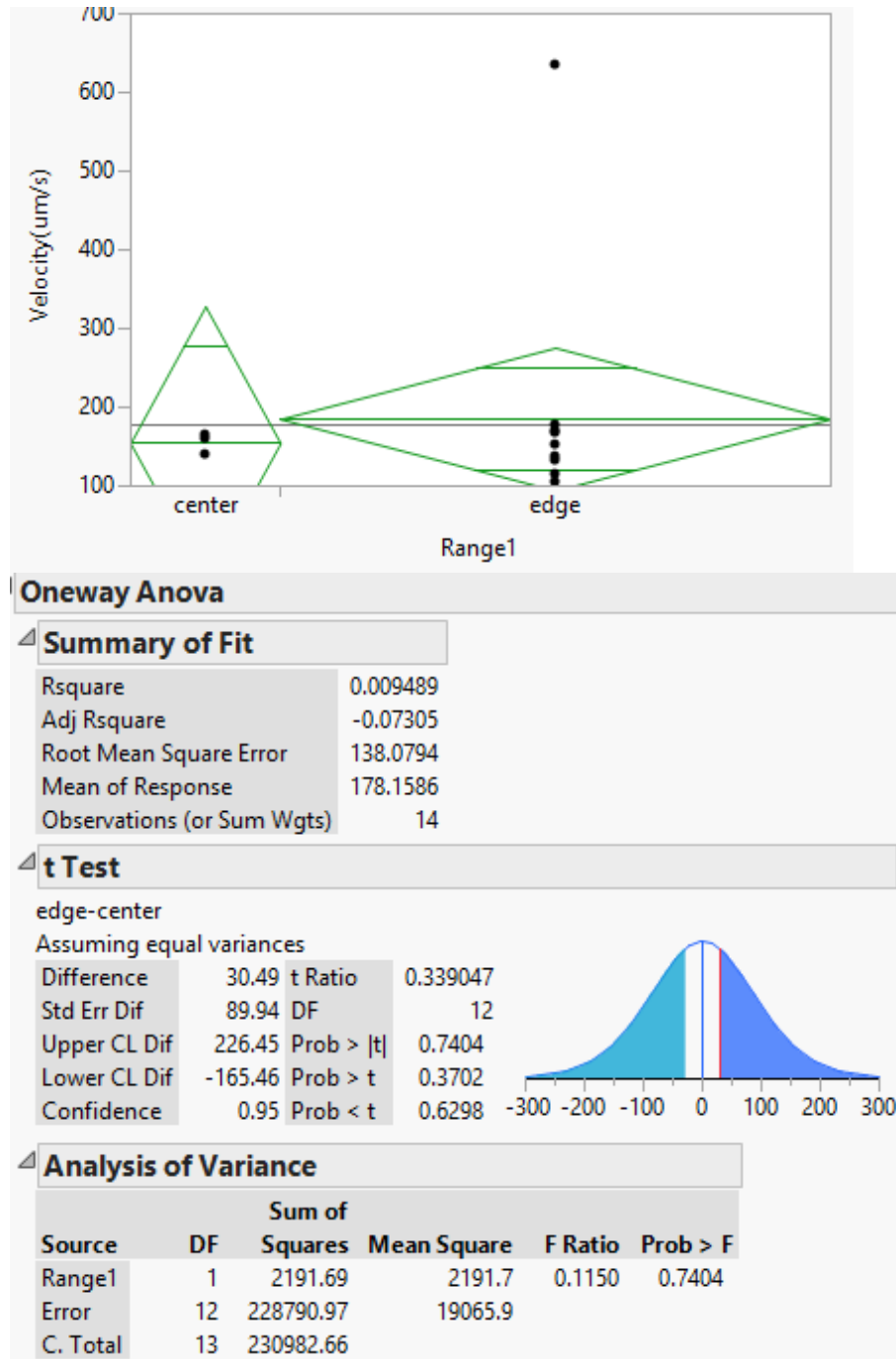


Figure 25 JMP output for 0.75 μ L/min of flow pressure. The edge is within 300 μ m of the wall. No significant difference between the regions of the channel was found.